Fluctuations in lifetime selection in an autocorrelated environment

Olivier Cotto, Luis-Miguel Chevin

HAL Id: hal-02998144
https://hal.science/hal-02998144

Submitted on 23 Nov 2020

FLUCTUATIONS IN LIFETIME SELECTION IN AN AUTOCORRELATED ENVIRONMENT

Olivier Cotto[1*] and Luis Miguel Chevin[1*]

1. Centre d'Ecologie Fonctionnelle et Evolutive Unité Mixte de Recherche 5175, Centre

National de la Recherche Scientifique–Université de Montpellier, Université Paul-Valéry

Montpellier, École Pratique des Hautes Études, 1919 route de Mende, 34293 Montpellier, Cedex

5, France.

Emails for correspondence *:

olivier.cotto2@gmail.com

luis-miguel.chevin@cefe.cnrs.fr

ABSTRACT

Most natural environments vary stochastically and are temporally autocorrelated. Previous theory

investigating the effects of environmental autocorrelation on evolution mostly assumed that total

fitness resulted from a single selection episode. Yet organisms are likely to experience selection

repeatedly along their life, in response to possibly different environmental states. We model the

evolution of a quantitative trait in organisms with non-overlapping generations undergoing several

episodes of selection in a randomly fluctuating and autocorrelated environment. We show that the

evolutionary dynamics depends not directly on fluctuations of the environment, but instead on

those of an effective phenotypic optimum that integrates the effects of all selection episodes within

each generation. The variance and autocorrelation of the integrated optimum shape the variance and predictability of selection, with substantial qualitative and quantitative deviations from previous predictions considering a single selection episode per generation. We also investigate the consequence of multiple selection episodes per generation on population load. In particular, we identify a new load resulting from within-generation fluctuating selection, generating the death of individuals without significance for the evolutionary dynamics. Our study emphasizes how taking into account fluctuating selection within lifetime unravels new properties of evolutionary dynamics, with crucial implications notably with respect to responses to global changes.

INTRODUCTION

32   The study of adaptation to changing environments has received renewed attention in the context

33   of current global changes induced by anthropogenic activities. Many theoretical studies on

34   adaptation to changing environments have focused on cases where environmental change follows

35   a deterministic trend (Lynch et al. 1991, Lynch and Lande 1993, Gomulkiewicz and Houle 2009,

36   Cotto and Ronce 2014), motivated by major tendencies such as climate warming. Yet, most

37   variation on short timescales results from stochastic fluctuations, and climatic time series generally

38   include stochastic variations around their main trends (Stocker et al. 2013). The variance and

39   autocorrelation of these fluctuations need to be modeled to accurately predict the impact of climate

40   warming on biosystems (e.g. Katz 1996, Rowell 2005). Global climatic dynamics have recently

41   been suggested to affect local selection pressures (Siepielski et al. 2017), and time series of

42   climatic variables are generally autocorrelated in time, notably as a result of thermic inertia

43   (Hasselmann 1976, Rowell 2005). As most climatic (and other ecologically relevant)

44   environmental variables are autocorrelated in time (Vasseur and Yodzis 2004), environmental

45   selective pressures are likely to also be temporally autocorrelated, an aspect that is often neglected

46   in models of adaptation that do include stochasticity in the environment (e.g. Lynch and Lande

47   1993, Engen et al. 2011, Engen et al. 2012).

48   Theoretical models of adaptation to stochastically changing environments often assume

49   that the fitness of an individual depends on the match between its phenotype and an optimum

50   phenotype influenced by the environment (so-called "moving optimum" models, reviewed by

51   Kopp and Matuszewski 2014). When the environment undergoes stationary stochastic

52   fluctuations, the effect of evolutionary responses on long-term fitness and expected population

53   growth depends on the variance and autocorrelation of changes in the optimum phenotype

54   (Charlesworth 1993, Lande and Shannon 1996, Chevin et al. 2017). If the stochastic fluctuations

55   of the optimum are not autocorrelated, then responses to selection in a given generation might

56   increase maladaptation in the next, with detrimental consequences for population growth (Lande

57   and Shannon 1996). In contrast, temporal autocorrelation of the optimum makes the environment

58   more predictable, such that the evolutionary response in a given generation is more likely to be

59   beneficial in the next, and that any factor improving the response to selection leads to a higher

60   expected long-term growth rate of the population (Lande and Shannon 1996, Chevin 2013). The

61   autocorrelation of the optimum also affects the variance and overall shape of the probability

62   distribution of population size of an evolving population, with consequences for extinction risk

63   (Chevin et al. 2017). Lastly, temporal autocorrelation of the environment is a major driver of the

64   evolution of plasticity, with higher reaction norm slopes evolving under more predictable

65   (autocorrelated) environments of selection (Gavrilets and Scheiner 1993, Lande 2009, Chevin et

66   al. 2015).

67   On the empirical side, a number of studies undertook to determine the temporal

68   characteristics of selection in natural populations. Temporal variation in selection is observed in

69   classic long-term surveys, like beak shape in Darwin's finches (Grant and Grant 2002), banding

70   patterns in Cepea snails (Cain et al. 1990) or spine number in threespined sticklebacks (Reimchen

71   and Nosil 2002, reviewed in Bell 2010). Consistent with these observations, studies analyzing

72   several datasets with long-term selection estimates using a common framework also found that

73   selection varies in strength and direction (Kingsolver and Diamond 2011, Siepielski et al. 2011,

74   but see Morrissey and Hadfield 2012). Further, the development of a statistical framework that

75   models temporal fluctuations in phenotypic selection as a random process, characterized by the

76   variance and autocorrelation of an optimum phenotype, allowed to show that the optimum laying

4

77 date in a population of Great tits undergoes autocorrelated temporal fluctuations (Chevin et al.

78 2015, Gamelon et al. 2018). This framework rests on a model of a Gaussian fitness peak, as in

79 many theoretical studies (Kopp and Matuszewski 2014), so that the estimated parameters should

80 have a direct theoretical interpretation.

81   However, the comparison of empirical measures of fluctuating selection with theoretical

82 results on adaptation to autocorrelated environment is an arduous task, because the definitions of

83 fitness and selection may not be easily transposed from one to the other. Even regardless of

84 theoretical considerations about the definition of long-term expected fitness in a stochastic

85 environment, understanding how variation in selection integrates within lifetime is not

86 straightforward. Most theoretical studies that included autocorrelation in the environment

87 neglected the dynamics of selection within generations, by assuming (often implicitly) that

88 selection occurs instantaneously, in discrete non-overlapping generations. In other word, lifetime

89 fitness is assumed to result from a single instantaneous episode of selection; or at least, the

90 unfolding of selection within lifetime is not modeled explicitly, making it ambiguous whether the

91 per-generation optimum represents instantaneous or repeated selection. More realistically,

92 selection occurs in several episodes along a generation (Lande 1982, Arnold and Wade 1984b). In

93 fact, the vast majority of long-term estimates of selection gradients focused on a single fitness

94 component (~ 98% among 2819 selection estimates in Kingsolver and Diamond 2011), and

95 therefore correspond to a single episode of selection, among several possible others in a generation

96 or lifetime. This has several related consequences for the interpretation of measurements of

97 selection. First, the strength of selection over a single episode cannot necessarily be compared to

98 predictions based on overall selection per generation, because this selection episode needs to be

99 weighted by its contribution to the lifetime (or per-generation / per-unit-time) fitness. Second, both

5

100 the magnitude and predictability of temporal variation in selection is probably not well captured

101 by treating each selection episode in isolation. The reason is that in organisms that undergo

102 multiple selection episodes, environmental variability gets integrated over lifetime. This has

103 important consequences, notably regarding the contribution of extreme events to selection, a topic

104 of recent interest (Grant et al. 2017, Marrot et al. 2017).

105   The study of demography has long questioned the relationship between variation in vital

106 rates that contribute to elements of the transition matrix (e.g. fecundities, survival rates) and

107 various measures of the population growth rate (Tuljapurkar et al. 2003, Morris et al. 2004, Saether

108 et al. 2013). This theory has been used to analyse fluctuating selection in stochastic environments

109 that are not autocorrelated (Engen et al. 2012, 2014). However, how stochastic autocorrelated

110 fluctuating selection mediated by different fitness components integrates over lifetime is an under-

111 investigated topic, limiting our understanding of adaptation to randomly changing environments.

112 Making progress on this question requires extending previous approaches that integrate the

113 multiplicity of selection episodes along life. Of particular note is the approach by Arnold and Wade

114 (1984b, 1984a), who proposed and applied a decomposition of lifetime selection into a series of

115 selection episodes with multiplicative effects on fitness, resulting in selection gradients (dependent

116 on log-fitness) that sum along a generation (see also McGlothlin 2010). Integrating the effect of

117 successive selection episodes on lifetime fitness is appropriate to organisms with non-overlapping

118 generations (Arnold and Wade 1984a), but has not been used to investigate the effect of

119 environmental stochasticity.

120   We here build a model of a phenotypic trait exposed to multiple selection episodes, in non-

121 overlapping generations. We assume that the phenotype of an individual at the focal trait does not

122 change between selection episodes. This could correspond for example to a morphological trait

123   that only influences selection after it is fully developed, or a coloration trait that affects survival

124   probability (due to e.g. predation, or thermoregulation) prior to reproduction. Under these

125   assumptions, we detail and clarify how the temporal structure of selection during lifetime

126   influences the predictability of lifetime viability selection, and the load caused by maladaptation

127   in a stochastic environment. Our model applies directly to organisms that are semelparous with

128   non-overlapping generations, including univoltine insects such as cicadas, and species with

129   economic or cultural significance such as salmons or bamboos. Our analysis further applies to

130   cohort analysis (see discussion) when considering more general life histories with overlapping

131   generations. As such, our study provides a necessary step toward a complete understanding of how

132   life history affects evolutionary dynamics in the context of autocorrelated fluctuating selection.

133   Overall, we find that the way selection operates during a lifetime strongly determines the impact

134   of environmental fluctuations on variation in selection across generations, and the incurred

135   maladaptation load in a stochastic environment.

136   MODEL

137 **Selection model**

138   We investigate the evolution of a single quantitative trait z in an organism with non-overlapping

139   generations. Along their life cycle, individuals undergo several selection episodes that determine

140   their probability to survive between stages before reproduction, with the latter occurring only at

141   the end of each generation. We further assume that there is no selection on fecundity, which we

142   denote B. For simplicity, we focused on a single trait, but our framework can be readily extended

143   to the multivariate case, with different (correlated) traits undergoing selection at different stages

144   (Arnold and Wade 1984b, Arnold and Wade 1984a, Cotto and Ronce 2014).

7

145   We further assume that the phenotype z at the beginning of a generation can be decomposed

146   as $z = x + e$, where x is the additive genetic value and e is a residual component of variation

147   independent of the additive genetic value, and with normal distribution of mean 0 and variance E

148   (Falconer and Mackay 1996). We assume that many loci contribute to the additive genetic value,

149   such that x is normally distributed with mean $\bar{x}$ and variance G. Under these assumptions, z is also

150   normally distributed with mean $\bar{z}$ and variance $P = G + E$.

151   The survival probability of an individual with phenotype z at age i in generation g depends

152   on the match between its phenotype z and an optimum phenotype $\theta_{g,i}$ that changes with the

153   environment,

154    $$W_{i,g}(z) = W_{max,i}\exp\left(-\frac{(z-\theta_{i,g})^2}{2\omega_{i,g}^2}\right). \tag{1}$$

155   where $W_{max,i}$ is the maximum survival rate at age i and ω_i measures the width of the Gaussian

156   survival function (inversely related to the strength of selection). We assume that selection occurs

157   through all transitions preceding reproduction, so that the components of fitness are multiplicative

158   (Arnold and Wade 1984a). If reproduction could occur at several stages, then the components of

159   fitness would no longer be multiplicative, and another framework (e.g. overlapping generations,

160   Charlesworth 1994) should be used. The total absolute fitness of an individual with phenotype z is

161   then (where the subscript g has been dropped for simplicity)

162    $$W(z) = B \prod_{i=1}^{n} W_i(z) \tag{2}$$

163   Under the assumption that selection is Gaussian at each episode (eq. 1), the total fitness function

164   is also Gaussian,

165    $$W(z) = W_{max,tot} \exp\left(-\frac{(z-\theta_{tot})^2}{2\omega_{tot}^2}\right), \tag{3}$$

8

where, $\omega_{tot}^2 = (\sum_i 1/\omega_i^2)^{-1}$ is the total strength of selection (that is the harmonic mean of the width of the selection function at each selection episode), $\theta_{tot} = \sum_i e_i \, \theta_i$ is the per-generation effective optimum corresponding to the sum of the phenotypic optima at each selection episode, weighted by the contribution of these episodes to the total strength of selection. We denote this contribution as $e_i = \frac{\omega_{tot}^2}{\omega_i^2}$, by reference to elasticities in stage-structured population models (Caswell 2001). The maximum absolute fitness over a generation is

$$W_{max,tot} = B \exp\left(-\frac{1}{2\omega_{tot}^2}\left(\sum_i e_i \, \theta_i^2 - (\sum_i e_i \, \theta_i)^2\right)\right)\prod_i W_{max,i}. \tag{4}$$

With the further assumption that the strength of selection (here measured as a width of the fitness function) is the same at all selection episodes, we have $\omega_i = \omega$ and $e_i = 1/n$, so the equations above further simplify as

$$\omega_{tot}^2 = \omega^2/n \tag{5}$$

$$\theta_{tot} = \frac{1}{n}\sum_k \theta_k = \widehat{E}[\theta] \tag{6}$$

$$W_{max,tot} = B \exp\left(-\frac{n\,\widehat{V}[\theta]}{2\omega^2}\right)\prod_i W_{max,i}, \tag{7}$$

where $\widehat{E}[\theta]$ and $\widehat{V}[\theta]$ are the "sample" expectation and variance (respectively) of θ within a generation.

The change in the mean phenotype over an entire generation, after reproduction, is (Lande 1976)

$$\Delta\bar{z} = h_0^2(\bar{z}_n - \bar{z}_0) = G_0 \frac{\partial \ln \overline{W}(z)}{\partial\bar{z}}, \tag{8}$$

where $\bar{z}_n$ is the mean phenotype after the last episode of selection, and additive genetic variance G_0 and heritability $h_0^2 = G_0/P_0$ are measured at the beginning of a generation, prior to any selection. Indeed, each selection event can generate a covariance between P and E that needs to be

9

187 accounted for if dealing with selection episode by episode (as in Arnold and Wade 1984a),

188 resulting in complications (see Supp. Mat.) that can be overcome by focusing on the effect on total

189 selection on the phenotype distribution prior to any selection. With Gaussian stabilizing selection

190 (eq. 1) and a normally distributed trait, the mean fitness in the population is

191 $\quad \overline{W}(\bar{z}) = \int p(z)W(z)dz = W_{max,tot}\sqrt{S_{tot}\omega_{tot}^2}\exp\left(-\frac{(\bar{z}-\theta_{tot})^2}{2(\omega_{tot}^2+P_0)}\right),$ (9)

192 where $S_{tot} = \frac{1}{P_0+\omega_{tot}^2}$. From equation 8, it follows that the per-generation change in the mean trait

193 value in the population is

194 $\quad \Delta\bar{z} = -G_0 S_{tot}(\bar{z} - \theta_{tot}) = -G_0\beta_{tot},$ (10)

195 where β_{tot} is the total selection gradient, and which has a similar form as in models with a single

196 selection episode (e.g. Lande 1976).

Fluctuations of the environment and timing of selection

198 We are interested in cases where the optimum phenotype fluctuates because of random fluctuations

199 in the environment, i.e. fluctuations of the optimum phenotype represent those of the environment.

200 For simplicity, we assume that the optimum phenotypes at all selection events in a life cycle

201 respond to the same environmental variable, so that fluctuations in the optimum during a lifetime

202 can be modeled as a temporal sampling of the same stochastic process. We consider the case where

203 the optimum follows a first-order autoregressive process with mean 0 (without loss of generality),

204 defined by

205 $\quad \theta_{t+1} = \rho\,\theta_t + \sigma_\theta\sqrt{1-\rho^2}\zeta_t$ (11)

206 where ρ is the autocorrelation of the optimum over one (absolute; e.g. one year) time unit (which

207 we assume is positive), σ_θ^2 its stationary stochastic variance, and ζ_t a standard normal random

208 deviate. For such a process, the autocorrelation of the optimum over k units of time is $\rho^k =$

209    $\exp(-k/T_\theta)$, where $T_\theta = -1/\ln(\rho)$ is the characteristic timescale of the autocorrelation of the

210   optimum. Note that the autoregressive process converges to white noise when ρ tends to 0, i.e.

211   when the optimum phenotype is correlated over an infinitesimally small timescale.

212   We assume that n episodes of selection occur before reproduction. These selection episodes

213   all take place over a time-window that spans a fraction α of generation time T. The time-window

214   for selection remains unchanged across generations. This models the fact that all traits in an

215   organism need not be exposed to selection throughout life. Instead, it is more likely that there is a

216   time-window within a generation during which a given trait may be sensitive to the environment

217   and exposed to selection (e.g. during the first stages). When exactly the time-window of selection

218   occurs within a generation (e.g. at the beginning or at the end) has no effect for the remaining of

219   the analysis. Under our assumption of non-overlapping generations, only the duration of this

220   window matters. For simplicity, we assume that the episodes of selection are evenly spaced along

221   the time-window for selection, so that they occur every $\alpha T/n$ units of time. Using the index g for

222   the number of generations, we denote as $\bar{z}_{g,0}$ the mean trait value before the first episode of

223   selection of generation g. The timescale of life history relative to that of the environment is

224   represented in figure 1.

225   RESULTS

226   **Predictability of selection**

227   The predictability of selection can be defined in several ways. For our purpose, we will focus on

228   the autocorrelation of the effective optimum per generation, and that of the total selection gradient,

229   because these relate to measurable quantities (Lande and Arnold 1983, Chevin et al. 2015,

230   Gamelon et al. 2019) known to affect adaptation and population dynamics in a stochastic

231   environment (Lande and Shannon 1996, Chevin 2013, Chevin et al. 2017). We first calculate the

232   autocorrelation of θ_{tot}, before investigating the properties of the fluctuations in the selection

233   gradient β_{tot}, which despite being less directly connected to theoretical predictions, are closer to

234   what is commonly estimated empirically (Lande and Arnold 1983).

235   *Autocorrelation of the effective optimum.*

236   The autocorrelation of the effective optimum at a lag of one generation is (see also Supp. Mat.)

237    $$\rho_{\theta tot} = \rho^T \frac{\sum_{k=1}^{n} e_k^2 + \sum_{i=1}^{n-1}\sum_{j=i+1}^{n} e_i e_j \rho^{(j-i)\alpha T/n}\left(1+\rho^{2(i-j)\alpha T/n}\right)}{\sum_{k=1}^{n} e_k^2 + 2\sum_{i=1}^{n-1}\sum_{j=i+1}^{n} e_i e_j \rho^{(j-i)\alpha T/n}} = \rho^T \varphi, \tag{12}$$

238   where ρ^T is the autocorrelation of the optimum over a generation time, and its autocorrelation

239   between two consecutive selection episodes is $\rho^{\alpha T/n}$ (which differs from the autocorrelation ρ

240   per time-unit). In the following we detail the inflating factor φ corresponding to the complex

241   fraction that appears in the first equality in equation (12). The first sum in the numerator results

242   from the covariance between the optimum in a given episode of selection and the same episode in

243   the next generation. The second sum results from the covariances of the optimum between two

244   different selection episodes in two consecutive generations. The denominator has a similar

245   structure, and results from similar effects (variance per episode *vs* covariance across episodes)

246   within a generation, contributing to the variance of the effective optimum (see Supp. Mat.). It can

247   be shown (by noting that $0 < \rho^{(j-i)\alpha T/n} \leq 1$, so that $\rho^{-(j-i)\alpha T/n} > 1$) that the ratio in equation

248   (12) is always larger than 1, and is thus an inflating factor, which always increases the

249   autocorrelation of the effective optimum relative to the autocorrelation of the environment, as a

250   results of the averaging of selection between episodes within generations. Remarkably, this result

251   extends to the autocorrelation over $\tau > 1$ generations when the autocorrelation of the environment

252   decreases exponentially with time, as occurs under a Markovian process such as our first-order

253 autoregressive process. We thus have for the autocorrelation of the effective optimum over $\tau \geq 1$

254 generations

255 $\rho_{\theta tot, \tau} = \rho^{\tau T} \varphi.$ (13)

256 Equation (13) shows that, once the inflation factor has been accounted for, the autocorrelation of

257 θ_{tot} declines exponentially at the same rate as the autocorrelation of θ (fig. 2A). In principle, then,

258 information on the autocorrelation of the effective optimum between two generations allows to

259 determine its autocorrelation over many generations, providing that the autocorrelation of the

260 environment (here also corresponding to the autocorrelation of θ) driving selection is known.

261 More insights arise from the simpler case where the strength of selection is the same at all

262 selection episodes (eq. 5-6), wherein φ simplifies to

263 $\varphi = \dfrac{\psi + \psi^{-1} - 2}{2(\psi - 1) + n(\psi^{-\frac{1}{n}} - \psi^{\frac{1}{n}})},$ (14)

264 where $\psi = \rho^{\alpha T}$ is the autocorrelation of θ over the time window for selection. Equation (14) shows

265 that when variance in the strength of stabilizing selection within generation can be neglected, then

266 the inflation factor does not depend on the strength of selection, but only on environmental

267 autocorrelation ψ over the time window for selection, and on the number of selection episodes.

268 The inflation factor φ increases when the autocorrelation of the environment decreases (fig. 2B,

269 C), and when the number of selection episode increases (fig. 2B). In other words, weakly

270 autocorrelated environments can actually correspond to much larger autocorrelations of variables

271 relevant to selection. For example, when there are many episodes of selection per generation and

272 the autocorrelation of the environment is 0.2, the autocorrelation of θ_{tot} can be increased by more

273 than 50% as compared to the autocorrelation of θ (fig. 2B). When the number of episodes of

274 selection is large, φ converges to

275 $$\varphi \xrightarrow{n\to\infty} \frac{(1-\psi)^2}{2\psi(\psi-\ln\psi-1)},$$ (15)

276 which only depends on environmental autocorrelation ψ over the time window for selection. We

277 found that equation (15) provides a good approximation for equation (13) as soon as there are more

278 than a few episodes of selection per generation, and even if the actual strength of selection varies

279 across episodes (fig. 2B). Interestingly, equation (15) does not depend on the strength of selection

280 at each episode, and proposes a simple transformation between the autocorrelation of the

281 environment and the autocorrelation of the effective optimum over a generation time. Substituting

282 equation (15) into equation (13) thus provides, in principle, a simple way to estimate the

283 autocorrelation of the effective optimum in natural populations from a measure of the

284 autocorrelation of the environment, over the duration of selection within a generation on one hand

285 (to compute the inflation factor), and across generations on the other hand. The longer the organism

286 is sensitive to selection within a generation, the larger the inflation factor (fig. 2C). Lastly, when

287 the environment is not autocorrelated, the effective optimum is not autocorrelated either, showing

288 that within-generation selection alone does not generate autocorrelation of the effective optimum.

289

290

291 *Fluctuations in directional selection.*

292 <u>Variance of the selection gradient</u>

293 Ultimately, evolutionary change in the mean phenotype in response to selection is directly related

294 to the total per-generation selection gradient β_{tot} (eq. 10). At stationarity after many generations,

295 we find that the variance of the selection gradient is approximately (see Supp. Mat.)

296 $$\mathrm{Var}[\beta_{tot}] \approx 2\,\mathrm{Var}[\theta_{tot}]S_{tot}^2 \frac{1-\rho^T\left(1+S_{tot}G_0(I_f-1)\right)}{(2-S_{tot}G_0)(1-\rho^T(1-S_{tot}G_0))}.$$ (16)

14

297 The variance of the selection gradient increases with the variance of fluctuations in the effective

298 optimum (and of the environment, see Supp. Mat.) and with the total strength of selection (eq. 16

299 and fig. 3). Equation (16) further shows that the variance of the selection gradient decreases when

300 the inflation factor increases. Correspondingly, $\text{Var}[\beta_{tot}]$ decreases with α (because the inflation

301 factor increases with α, fig. 2C) and with the number of selection episodes (fig. 2B and 3A). In

302 other words, recurrent selection along a generation tends to decrease the variance of the selection

303 gradient, as expected since environmental variation is averaged among selection episodes.

304 Less expected is the effect of environmental autocorrelation. We find that with several selection

305 episodes per generation, the variance of the selection gradient depends non-monotonically on the

306 autocorrelation of the environment, with a maximum when the environment is moderately

307 autocorrelated (fig. 3B). This result contrasts with the case with a single selection episode per

308 generation, where the variance in the selection gradient decreases with increasing autocorrelation

309 of the environment, as a result of better adaptive tracking of the optimum (Lande and Shannon

310 1996, Chevin and Haller 2014). This difference arises because, with several episodes of selection,

311 positive autocorrelation in the environment not only produces autocorrelation of the total optimum

312 θ_{tot} across generations, but also increases the variance of θ_{tot} (see eq. A1 and fig. A1 in Supp.

313 Mat.), with antagonistic effects on adaptive tracking by genetic evolution, and hence on the

314 variance of the total selection gradient across generations (Lande and Shannon 1996, Chevin and

315 Haller 2014).

316 We also investigated the influence of variable selection strength, by comparing the variance of the

317 selection gradient obtained for a fixed strength of selection per episode (eq. 5-6) with the case

318 where the strength of selection is drawn randomly at each episode from a distribution with the

319 same expected total selection S_{tot} (details in fig. 2 caption). We found that when there are only few

320   episodes of selection per generation, variance in total selection per generation increases the

321   variance of the selection gradient relative to what is expected in the deterministic case. However,

322   with many selection episodes per generation, the variance in total selection decreases, resulting in

323   a good fit between the simulations and the deterministic expectation (fig. 3, compare crosses with

324   dashed lines and circles). The effect of random selection per generation increases when selection

325   is strong (fig. 3). Lastly, we compared predictions from equation (16) calculated from a discrete

326   generation model to previous results using a continuous time approximation (Lande and Shannon

327   1996 eq. 7 and table 1, and Chevin and Haller 2014 eq. 5a). The continuous time approximation

328   provides more compact equations but tends to underestimate the variance of the selection gradient

329   when selection increases (fig. 3, compare dashed and continuous lines).

330

331

332   <u>Autocorrelation of the selection gradient</u>

333   For the autocorrelation function of the total selection gradient across generations, we start by

334   analyzing its expression in the case of a single selection episode per generation (i.e. when $\varphi = 1$).

335   We obtain (see Supp. Mat.) for selection gradients τ generations apart

336    $\rho_{\beta tot, \tau | n=1} = \frac{\rho^{\tau T} - \kappa (1 - S_{tot} G_0)^\tau}{1 - \kappa},$ $\qquad\qquad\qquad$ (17)

337   where $\kappa \approx S_{tot} G_0 \frac{(1+\rho^T)}{2(1-\rho^T)}$ (see eq. A15). Equation (17) is similar in form to an expression obtained

338   previously using a continuous-time approximation (eq. 5a in Chevin and Haller 2014), and leads

339   to similar conclusions. The autocorrelation of the selection gradient with one selection episode is

340   a linear combination of two exponentially decreasing functions, corresponding on the one hand to

341   the autocorrelation of the environment (first term in numerator), and to evolutionary responses to

16

342   deviations from the optimum (second term in the numerator) on the other hand. Consistent with

343   the result of Chevin and Haller (2014), we find that for large autocorrelation in the environment,

344   equation (17) converges to $(1 - S_{tot} G_0)^\tau$, demonstrating that inertia in responses to selection sets

345   an upper limit to the autocorrelation of the selection gradient.

346   In the general case where selection can occur in several episodes within a generation, we

347   find a more complex expression for the autocorrelation of the selection gradient, which can

348   nevertheless still be written in the form

349    $\rho_{\beta tot,\tau} = \frac{\varphi \varepsilon \rho^{\tau T} + \gamma (1 - S_{tot} G_0)^\tau}{\vartheta}$,   (18)

350   where the detailed expressions of ε, γ and ϑ depend on the per-generation evolutionary potential

351    $S_{tot} G_0$, the autocorrelation of the environment over a generation ρ^T, and γ and ϑ depend

352   additionally on the inflation factor φ. The details of these terms can be found in the calculations

353   provided in supplementary material (eq. A14). Equations (17) and (18) provide general

354   expressions for the autocorrelation of the selection gradient with discrete generations and multiple

355   selection episodes, extending previous results that used a continuous-time approximation with a

356   single episode (Chevin and Haller 2014).

357   Comparing equations (17) and (18) highlights that with multiple selection episodes, the

358   autocorrelation of the environment ρ and the rate of response to selection $S_{tot} G_0$ do not have in

359   general an additive influence on the autocorrelation of selection gradients across generations,

360   because the factor φ multiplying the former depends on the latter, and reciprocally for γ. This

361   occurs because with multiple episodes of selection, the relevant autocorrelation is that of the

362   effective optimum, which integrates the effect of selection across *and within* generations. The

363   autocorrelation of the selection gradient increases most with the number of selection episodes

364   when the autocorrelation of the environment is low (fig. 4A), consistent with what we found for

17

365   the inflation factor (fig. 2B and eq. 18). We also find that for a given number of selection episodes

366   per generation, the autocorrelation of the selection gradient slightly decreases when the total

367   strength of selection increases (fig. 4B).

368   Over time intervals longer than a generation, the autocorrelation function of selection

369   gradients for a single selection episode (eq. 17) and for multiple episodes (eq. 18) have a similar

370   shape (fig. 5), because they depend on the autocorrelation of the environment and of the effective

371   optimum (respectively), which have the same exponential rate of decrease (fig. 2A). Importantly

372   however, the autocorrelation of βtot in the first few generations - where the effect of multiple

373   episodes is most pronounced - weights most in determining the expected maladaptation in a given

374   generation (see e.g. eq. A6 in Supp. Mat.), so that differences in autocorrelation over short intervals

375   of generations can have profound effects. It is worth mentioning that equations (17) and (18) can

376   produce negative autocorrelations (fig. 5) when the effect of the evolutionary inertia (second term

377   at the numerator) grows larger that the effect of the autocorrelation of environment (see also

378   Chevin and Haller 2014).

379   Lastly, and similarly to the variance of the selection gradient, we found that when the

380   strength of selection is drawn randomly at each selection episode (see previous related paragraph

381   for variance), the autocorrelation of selection is below its expectation under constant selection

382   strength, when there are only few selection episodes per generation (fig. 4A). This difference is

383   especially marked when the environment is very autocorrelated and when selection is strong (fig.

384   4A, B) and vanishes as the number of selection episodes per generation increases.

385

Maladaptation load

Much of the work on adaptation of quantitative traits to autocorrelated stochastic environments has focused on the resulting expected lag load caused by deviations of the mean phenotype from the optimum, as this directly connects to long-term population growth and extinction risk (Lande and Shannon 1996, Chevin et al. 2017). From equation (10), the log mean fitness in the population (which relates to the relative increase in population size) is

$$\ln\overline{W} = r_{max} - \frac{1}{2\omega_{tot}^2}[\textstyle\sum_k e_k \theta_k^2 - (\sum_k e_k \theta_k)^2] - \frac{1}{2}\ln\left(1 + \frac{P_0}{\omega_{tot}^2}\right) - \frac{S_{tot}}{2}(\bar{z} - \theta_{tot})^2 \qquad (19)$$

where $r_{max} = \ln B + \sum_{k=1}^{n} r_{max,k}$ corresponds to the maximum potential fitness, for a hypothetical population that would be monomorphic for the optimal phenotype in each selection episode. The last two terms describe reductions in fitness caused by maladaptation of the mean phenotype and phenotypic variance in the population, as described in the literature (Lande and Shannon 1996). When considering several selection episodes per generation, there is an additional load that is directly linked to the fluctuations in the optimum (second term in eq. 19). Indeed, this load vanishes when the optimum does not fluctuate across episodes ($\theta_k = \theta$ for all k). It thus corresponds to the deaths of individuals induced by environmental fluctuations within a generation, which reduce population growth without evolutionary significance. Note that when the trait has phenotypic variance, the mean phenotype does change under selection within a generation, tracking the optimum phenotype to some extent following each selection episode. But each of these selection episodes requires a number of selective deaths, and the resulting total cost of natural selection (sensu Haldane 1957) over a generation is unaffected by phenotypic tracking: the load is exactly the same if there is no phenotypic variation, and no within-generation phenotypic tracking. When the strength of selection at each episode ω is constant (corresponding to eq. 5), we further have

$$\frac{1}{2\omega_{tot}^2}[\textstyle\sum_k e_k \theta_k^2 - (\sum_k e_k \theta_k)^2] = \frac{n\,\hat{\mathbb{V}}[\theta]}{2\omega^2}, \qquad (20)$$

19

409   such that the intra-generational load is proportional to the sample variance $\widehat{V}[\theta]$ of the optimum

410   across selection episodes within a generation.

411   In models of selection with a Gaussian fitness peak, there is a simple connection between

412   the temporal distribution of the directional selection gradients and the expected maladaptation

413   affecting populations growth, since both depend on the expected squared mismatch of the mean

414   phenotype from the optimum (Chevin and Haller 2014), $y = \bar{z} - \theta_{tot}$. The expected maladaptation

415   load L_m, defined as the decrease in log mean fitness induced by a mismatch between the population

416   mean and the optimum phenotype, is $E[L_m] = \frac{S}{2} E[(\bar{z} - \theta_{tot})^2] = \frac{S}{2} \text{Var}[y]$ in a stationary

417   stochastic environment, and the variance of the selection gradient is $Var[\beta_{tot}] = S_{tot}^2 Var[y]$ (eq.

418   A5), leading to the simple relationship $E[L_m] = \text{Var}[\beta_{tot}]/(2S_{tot})$. The maladaptation load in a

419   fluctuating environment thus increases with the variance of the selection gradient and decreases

420   with the total strength of selection. In particular, in an autoregressive environment where several

421   selection episodes can occur within generations, we find that

422    $\text{E}[L_m] = \text{Var}[\theta_{tot}]S_{tot}\dfrac{1-\rho^T\left(1+S_{tot}G_0(I_f-1)\right)}{(2-S_{tot}G_0)(1-\rho^T(1-S_{tot}G_0))}$ (21)

423   The first term in equation (21) shows that the expected component of the maladaptation load

424   affected by responses to selection increases with the variance of the effective optimum (weighted

425   by the strength of selection). The maladaptation load changes non-monotonically as a function of

426   the autocorrelation of the environment (fig. 6A), as does the variance of the total selection gradient

427   (fig 3A). Total maladaptation is strongest at intermediate autocorrelation of the environment (fig.

428   6A), contrary to the case of a single selection episode. Furthermore, the expected maladaptation

429   decreases with increasing number of selection episodes within generation (fig. 6B), because this

430   decreases the variance of the effective optimum, and in turn the variance of the selection gradient

431   (see Supp. Mat. and fig. A1). However, note that this decreased variance of the effective optimum

432   come at the expense of an increased load of fluctuating selection within a generation, which cannot

433   be overcome by adaptive tracking.

434

435   DISCUSSION

436   Most theoretical studies investigating the effect of an autocorrelated environment on evolutionary

437   dynamics and their consequences for population dynamics assumed simple life cycles, where the

438   timing of selection within a generation was left implicit (e.g. Charlesworth 1993, Lande and

439   Shannon 1996, Chevin 2013). In models of non-overlapping generations, the timing of life-history

440   events is generally not addressed, and selection is most often modeled as a single, effectively

441   instantaneous process. This contrasts with the fact that many traits are likely to affect fitness at

442   different times in life, and thus undergo several episodes of selection (Arnold and Wade 1984b,

443   Marshall and Morgan 2011). Another difficulty at the interface of theory and empirical work on

444   these questions is that measuring fitness is in practice challenging, such that natural selection is

445   mostly estimated in the form of individual selection episodes acting via specific fitness

446   components in the life cycle (Kingsolver and Diamond 2011, Siepielski et al. 2017). Recent

447   refinements (e.g. McGlothlin 2010) of theory on the measurement of selection gradient (Lande

448   and Arnold 1983, Arnold and Wade 1984a, Wade and Kalisz 1989) investigated how estimates of

449   selection at different episodes within a generation can be integrated to infer overall selection, and

450   the resulting evolutionary response. The present study extends this theory by investigating how

451   fluctuating selection resulting from changes in the environment within and across generations

452   impacts evolutionary trajectories, and the potential for population persistence.

453   To this aim, we developed a model of an organism with non-overlapping generations,

454   where several transitions between stages (survival) prior to reproduction depend on the match

455   between a phenotypic trait and a fluctuating optimal value directly related to the environment,

456   consistent with recent empirical estimates of fluctuating selection in the form of a moving

457   phenotypic optimum (Chevin et al. 2015, Gamelon et al. 2019). Our analysis of this model

458   demonstrates that knowledge of fluctuation patterns for the environment affecting selection is not

459   sufficient to infer the predictability of selection across generations, when there are multiple

460   selection episodes per generation. Selection across generations depends on an integrated optimum

461   that includes the relative contribution of each selection episode to total selection along the life

462   cycle, similar to recent formulations for age-structured populations but without autocorrelation

463   (Engen et al. 2011, Cotto et al. 2019). Therefore, fluctuations of selection across generations

464   depend on the pattern of variance and autocorrelation of the effective optimum, rather than of the

465   environment *per se*. One of our main results is that, when the environment undergoes red noise

466   (first-order autoregressive process), fluctuating selection within a generation causes the

467   autocorrelation of the effective optimum to be inflated relative to the autocorrelation of the

468   environment. We show that as the number of selection episode per generation increases, the

469   inflation factor rapidly converges to an asymptotic value that depends neither on the number of

470   episodes of selection nor on the strength of selection, but only on the autocorrelation of the

471   environment over a time window of selection. This asymptotic value can be used in practical

472   situations to estimate the autocorrelation of the effective optimum directly from measurement of

473   the autocorrelation of the environment. Importantly, however, this result depends on the

474   assumption that total selection (or its expectation) does not depend on the number of selection

475   episodes per generation. This assumption allows us to disentangle the effect of selection acting

476   repetitively along a generation from the effect of stronger total selection. We emphasize that this

477   independence may not be satisfied in natural populations, where more selection episodes may often

478   cause stronger overall selection.

479   The inflation factor for the optimum directly influences the autocorrelation of directional

480   selection gradients, which relates more directly to empirical measurements of the predictability

481   and consistency of directional selection through time (Grant and Grant 2002, Morrissey and

482   Hadfield 2012). However, an important point when considering the connection with empirical

483   work is that, instead of tracking phenotypic change under selection episode per episode as done

484   empirically (Arnold and Wade 1984b, McGlothlin 2010), we combined all episodes to derive a

485   total per-generation individual fitness function. This allowed us to elude the difficulties arising

486   from the dynamics of variances and covariances of breeding and phenotypic values at each

487   successive episode of selection (see Supp. Mat. for the calculations per-episode). Indeed, the

488   quantitative genetics framework assumes that genetic and environmental values are independent

489   prior to selection. It is no longer the case after the first episode of selection within a generation

490   (prior to reproduction), which generates a covariance between the above components. Tracking

491   changes in the mean phenotype and breeding values across selection episodes therefore requires

492   taking into account the change in covariance between breeding value and environmental values

493   (See. Supp. Mat. for a demonstration). The buildup of this covariance complicates the investigation

494   at the scale of individual selection episodes, from both a theoretical and empirical point of view

495   (Wade and Kalisz 1989, Cam et al. 2002, McGlothlin 2010), because the selection gradients are

496   no longer sufficient to describe accurately the change in the mean breeding value.

497   We also found that allowing for multiple selection episodes complicates the connection

498   between environmental autocorrelation and the variance of selection gradients, which is directly

499   linked to the expected maladaptation load reducing population growth (Chevin et al. 2017). With

500   multiple selection episodes, both these metrics vary non-monotonically with the autocorrelation of

501   the environment, with a maximum at an intermediate value. This contrasts with previous results

502   from models with a single episode of selection per generation, where the expected maladaptation

503   load decreases monotonically with increasing autocorrelation of the environment, because this

504   allows for closer adaptive tracking of the moving optimum via genetic evolution (Chevin 2013,

505   Chevin et al. 2015). That this may not hold with multiple episodes of selection crucially revises

506   previous understanding of the role of environmental autocorrelation on maladaptation:

507   maladaptation can actually increase with increasing autocorrelation of the environment.

508   Lastly, we found that selection that fluctuates within a generation results in a specific load,

509   which adds up to the maladaptation and variance loads classically described in the literature on

510   adaptation to changing environments (see Lynch and Lande 1993, Burger and Lynch 1995, Lande

511   and Shannon 1996, Kopp and Matuszewski 2014). This load only exists when the direction and/or

512   strength of selection varies within a generation, and also increases with the number of selection

513   episodes and the total per-generation strength of selection. The reason for this load is that each

514   selection episode results in selective deaths that reduce the demographic output of the population,

515   as previously discussed in extensions of Haldane's (1957) famous "cost of natural selection" to

516   the context of adaptation to a changing environment, with a single selection episode (Nunney

517   2003). Within-generation fluctuations in selection increase this number of selective deaths without

518   any net beneficial effect on adaptation: from an evolutionary perspective, individuals are

519   essentially wasted by within-generation fluctuation in selection. An important implication of this

520   result is that disturbances that increase temporal variation in the environment can lead to the

521   decline of a population, regardless of its phenotypic state (mean phenotype, additive genetic

522   variance). This bears particular importance in light of the increasing frequency of extreme climatic

523 events (Coumou and Rahmstorf 2012), and accumulating evidence of their effect on evolutionary

524 and demographic dynamics (Moreno and Møller 2011, Marrot et al. 2017). This load caused by

525 fluctuating selection within a generation may only be alleviated by mechanisms that cause within-

526 generation adaptive changes in the mean phenotype without requiring any selective death. This

527 suggests that a powerful mechanism by which labile, reversible plasticity can evolve (as

528 investigated theoretically in a few studies, Gabriel 2005, Lande 2014, Ratikainen and Kokko 2019)

529 is by reducing the load caused by fluctuating selection within a generation.

530   Our non-overlapping generation model applies directly to univoltine species. An

531 interesting extension would be to investigate the case with overlapping generations. The most

532 closely related life cycle with overlapping generations is that of perennial semelparous organisms,

533 encompassing a large diversity of organisms (Young and Augspurger 1991) spanning from

534 microbial parasites (Ebert and Weisser 1997) to long lived plants (e.g. semelparous yucca) and

535 vertebrates (e.g. pacific salmon). This type of life cycle can lead to asynchrony in reproduction

536 among age classes (Caswell 2001 p.81-88), such that the population at any time is composed of

537 cohorts with different ages that rarely interbreed, in which case our conclusions directly apply to

538 each of these cohorts. Perennial semelparous life cycles can also produce instability in age

539 structure, which has been proposed to contribute to periodicity in species such as cicadas (Bulmer

540 1977) or bamboos (Keeley and Bond 1999). This instability may even lead to a collapse of age

541 structure and to a synchrony in reproduction (Mjølhus et al. 2005), in which case our model would

542 apply to the entire population. In contrast, iteroparity in perennial organisms would add

543 considerable complications to the investigation of the effects of fluctuations in the environment.

544 Indeed, each cohort of offspring is contributed from cohorts of reproductive individuals having

25

545   experienced different history of selection, possibly generating deviations from the stable (st)age

546   structure (see Lorimer 1980 for an example). We leave such an investigation for a future study.

547   REFERENCES

548   Arnold, S. J., and M. J. Wade. 1984a. On the measurement of natural and sexual selection - theory.

549   Evolution **38**:709-719.

550   Arnold, S. J., and M. J. Wade. 1984b. On the measurement of natural and sexual selection:

551   applications. Evolution **38**:720-734.

552   Bell, G. 2010. Fluctuating selection: the perpetual renewal of adaptation in variable environments.

553   Philos Trans R Soc Lond B Biol Sci **365**:87-97.

554   Bulmer, M. 1977. Periodical insects. The American Naturalist **111**:1099-1117.

555   Burger, R., and M. Lynch. 1995. Evolution and extinction in a changing environment: a

556   quantitative-genetic analysis. Evolution:151-163.

557   Cain, A. J., L. Cook, and J. D. Currey. 1990. Population size and morph frequency in a long-term

558   study of Cepaea nemoralis. Proc. R. Soc. Lond. B **240**:231-250.

559   Cam, E., W. A. Link, E. G. Cooch, J.-Y. Monnat, and E. Danchin. 2002. Individual covariation in

560   life-history traits: seeing the trees despite the forest. The American Naturalist **159**:96-105.

561   Caswell, H. 2001. Matrix population models. Sinauer Associates Sunderland, Massachusetts,

562   USA.

563   Charlesworth, B. 1993. Directional selection and the evolution of sex and recombination. Genetics

564   Research **61**:205-224.

565   Charlesworth, B. 1994. Evolution in age-structured populations. Cambridge University Press

566   Cambridge.

567   Chevin, L.-M., O. Cotto, and J. Ashander. 2017. Stochastic Evolutionary Demography under a

568   Fluctuating Optimum Phenotype. The American Naturalist **190**:786-802.

569   Chevin, L. M. 2013. Genetic constraints on adaptation to a changing environment. Evolution

570   **67**:708-721.

571   Chevin, L. M., and B. C. Haller. 2014. The temporal distribution of directional gradients under

572   selection for an optimum. Evolution **68**:3381-3394.

573   Chevin, L. M., M. E. Visser, and J. Tufto. 2015. Estimating the variation, autocorrelation, and

574   environmental sensitivity of phenotypic selection. Evolution **69**:2319-2332.

575   Cotto, O., and O. Ronce. 2014. Maladaptation as a source of senescence in habitats variable in

576   space and time. Evolution **68**:2481-2493.

577   Cotto, O., L. Sandell, L.-M. Chevin, and O. Ronce. 2019. Maladaptive Shifts in Life History in a

578   Changing Environment. The American Naturalist **194**:000-000.

579   Coumou, D., and S. Rahmstorf. 2012. A decade of weather extremes. Nature Climate Change

580   **2**:491.

581   Ebert, D., and W. W. Weisser. 1997. Optimal killing for obligate killers: the evolution of life

582   histories and virulence of semelparous parasites. Proceedings of the Royal Society of

583   London. Series B: Biological Sciences **264**:985-991.

584   Engen, S., R. Lande, and B. E. Saether. 2011. Evolution of a plastic quantitative trait in an age-

585   structured population in a fluctuating environment. Evolution **65**:2893-2906.

586   Engen, S., B. E. Saether, T. Kvalnes, and H. Jensen. 2012. Estimating fluctuating selection in age-

587   structured populations. J Evol Biol **25**:1487-1499.

588   Falconer, D., and T. Mackay. 1996. Introduction to quantitative genetics. 1996. Harlow, Essex,

589   UK: Longmans Green **3**.

27

590   Gabriel, W. 2005. How stress selects for reversible phenotypic plasticity. Journal of Evolutionary

591   Biology **18**:873-883.

592   Gamelon, M., Tufto, J., Nilsson, A. L., Jerstad, K., Røstad, O. W., Stenseth, N. C., & Sæther, B.

593   E. (2018). Environmental drivers of varying selective optima in a small passerine: A

594   multivariate, multiepisodic approach. Evolution, 72(11), 2325-2342.

595   Gamelon, M., S. J. Vriend, S. Engen, F. Adriaensen, A. A. Dhondt, S. R. Evans, E. Matthysen, B.

596   C. Sheldon, and B. E. Sæther. 2019. Accounting for interspecific competition and age

597   structure in demographic analyses of density dependence improves predictions of

598   fluctuations in population size. Ecology Letters.

599   Gavrilets, S., and S. M. Scheiner. 1993. The genetics of phenotypic plasticity. V. Evolution of

600   reaction norm shape. Journal of Evolutionary Biology **6**:31-48.

601   Gomulkiewicz, R., and D. Houle. 2009. Demographic and Genetic Constraints on Evolution.

602   American Naturalist **174**:E218-E229.

603   Grant, P. R., and B. R. Grant. 2002. Unpredictable evolution in a 30-year study of Darwin's finches.

604   Science **296**:707-711.

605   Grant, P. R., B. R. Grant, R. B. Huey, M. T. Johnson, A. H. Knoll, and J. Schmitt. 2017. Evolution

606   caused by extreme events. Phil. Trans. R. Soc. B **372**:20160146.

607   Haldane, J. B. S. 1957. The cost of natural selection. Journal of Genetics **55**:511.

608   Hasselmann, K. 1976. Stochastic climate models part I. Theory. tellus **28**:473-485.

609   Katz, R. W. 1996. Use of conditional stochastic models to generate climate change scenarios.

610   Climatic Change **32**:237-255.

611   Keeley, J. E., and W. J. Bond. 1999. Mast flowering and semelparity in bamboos: the bamboo fire

612   cycle hypothesis. The American Naturalist **154**:383-391.

613   Kingsolver, J. G., and S. E. Diamond. 2011. Phenotypic selection in natural populations: what

614   limits directional selection? The American Naturalist **177**:346-357.

615   Kopp, M., and S. Matuszewski. 2014. Rapid evolution of quantitative traits: theoretical

616   perspectives. Evolutionary Applications **7**:169-191.

617   Lande, R. 1976. Natural selection and random genetic drift in phenotypic evolution. Evolution

618   **30**:314-334.

619   Lande, R. 1982. A quantitative genetic theory of life history evolution. Ecology:607-615.

620   Lande, R. (2007). Expected relative fitness and the adaptive topography of fluctuating selection.

621   Evolution, 61(8), 1835-1846.

622   Lande, R. 2009. Adaptation to an extraordinary environment by evolution of phenotypic plasticity

623   and genetic assimilation. Journal of Evolutionary Biology **22**:1435-1446.

624   Lande, R. 2014. Evolution of phenotypic plasticity and environmental tolerance of a labile

625   quantitative character in a fluctuating environment. J Evol Biol **27**:866-875.

626   Lande, R., and S. J. Arnold. 1983. The measurement of selection on correlated characters.

627   Evolution **37**:1210-1226.

628   Lande, R., and S. Shannon. 1996. The role of genetic variation in adaptation and population

629   persistence in a changing environment. Evolution **50**:434-437.

630   Lorimer, C. G. 1980. Age structure and disturbance history of a southern Appalachian virgin forest.

631   Ecology **61**:1169-1184.

632   Lynch, M., W. Gabriel, and A. M. Wood. 1991. Adaptive and demographic responses of plankton

633   populations to environmental-change. Limnology and Oceanography **36**:1301-1312.

634   Lynch, M., and R. Lande. 1993. Evolution and extinction in response to environmental change.

635   Biotic interactions and global change:234-250.

636   Marrot, P., D. Garant, and A. Charmantier. 2017. Multiple extreme climatic events strengthen

637   selection for earlier breeding in a wild passerine. Phil. Trans. R. Soc. B **372**:20160372.

638   Marshall, D. J., and S. G. Morgan. 2011. Ecological and evolutionary consequences of linked life-

639   history stages in the sea. Current Biology **21**:R718-R725.

640   McGlothlin, J. W. 2010. Combining selective episodes to estimate lifetime nonlinear selection.

641   Evolution **64**:1377-1385.

642   Mjølhus, E., A. Wikan, and T. Solberg. 2005. On synchronization in semelparous populations.

643   Journal of Mathematical Biology **50**:1-21.

644   Moreno, J., and A. P. Møller. 2011. Extreme climatic events in relation to global change and their

645   impact on life histories. Current Zoology **57**:375-389.

646   Morris, W. F., & Doak, D. F. (2004). Buffering of life histories against environmental

647   stochasticity: accounting for a spurious correlation between the variabilities of vital rates

648   and their contributions to fitness. The American Naturalist, 163(4), 579-590.

649   Morrissey, M. B., and J. D. Hadfield. 2012. Directional selection in temporally replicated studies

650   is remarkably consistent. Evolution **66**:435-442.

651   Nunney, L. 2003. The cost of natural selection revisited. Pages 185-194 *in* Annales Zoologici

652   Fennici. JSTOR.

653   Ratikainen, I. I., and H. Kokko. 2019. The coevolution of lifespan and reversible plasticity. Nature

654   Communications **10**:538.

655   Reimchen, T., and P. Nosil. 2002. Temporal variation in divergent selection on spine number in

656   threespine stickleback. Evolution **56**:2472-2483.

657   Rowell, D. P. 2005. A scenario of European climate change for the late twenty-first century:

658   seasonal means and interannual variability. Climate Dynamics **25**:837-849.

659 Engen, S., Sæther, B. E., Kvalnes, T., & Jensen, H. (2012). Estimating fluctuating selection in age-

660   structured populations. Journal of evolutionary biology, 25(8), 1487-1499.

661 Engen, S., Kvalnes, T., & Sæther, B. E. (2014). Estimating phenotypic selection in age-structured

662   populations by removing transient fluctuations. Evolution, 68(9), 2509-2523.

663 Engen, S., Sæther, B. E., Armitage, K. B., Blumstein, D. T., Clutton-Brock, T. H., Dobson, F. S.,

664   Festa-Bianchet, M., Oli, M. K. , Ozgul, A. (2013). Estimating the effect of temporally

665   autocorrelated environments on the demography of density-independent age-structured

666   populations. Methods in Ecology and Evolution, 4(6), 573-584.

667 Siepielski, A. M., J. D. DiBattista, J. A. Evans, and S. M. Carlson. 2011. Differences in the

668   temporal dynamics of phenotypic selection among fitness components in the wild.

669   Proceedings of the Royal Society of London B: Biological Sciences **278**:1572-1580.

670 Siepielski, A. M., M. B. Morrissey, M. Buoro, S. M. Carlson, C. M. Caruso, S. M. Clegg, T.

671   Coulson, J. DiBattista, K. M. Gotanda, and C. D. Francis. 2017. Precipitation drives global

672   variation in natural selection. Science **355**:959-962.

673 Stocker, T. F., D. Qin, G.-K. Plattner, M. Tignor, S. K. Allen, J. Boschung, A. Nauels, Y. Xia, V.

674   Bex, and P. M. Midgley. 2013. Climate change 2013: The physical science basis.

675   Cambridge University Press Cambridge.

676 Tuljapurkar, S., Horvitz, C. C., & Pascarella, J. B. (2003). The many growth rates and elasticities

677   of populations in random environments. The American Naturalist, 162(4), 489-502.

678 Vasseur, D. A., and P. Yodzis. 2004. The color of environmental noise. Ecology **85**:1146-1152.

679 Wade, M. J., and S. Kalisz. 1989. The additive partitioning of selection gradients. Evolution

680   **43**:1567-1569.

681   Young, T. P., and C. K. Augspurger. 1991. Ecology and evolution of long-lived semelparous

682   plants. Trends in Ecology & Evolution **6**:285-289.

683

FIGURE CAPTIONS

685

686 Figure 1: Schematic representation of the timescales and autocorrelation measures. Generations

687 last T units of time, within which selection occurs in n selection episodes spread over αT units of

688 time. The autocorrelation of the optimum phenotype (which is identical to that of the environment)

689 over the within-generation time of selection is $\psi = \rho^{\alpha T}$, and over a generation time is ρ^T. The per-

690 generation effective optimum integrates the effect of selection within generations. We denote $\rho_{\theta_{tot}}$

691 the autocorrelation of this measure over a generation. The schema highlights that the variance and

692 autocorrelation differ between the optimum phenotype at each episode of selection (i.e. the

693 environment) and the effective optimum relevant for the evolutionary dynamics across

694 generations.

695

696 Figure 2: Autocorrelation of the effective optimum and inflation factor. Panel A: Autocorrelation of the effective

697 optimum as a function of the number of generations for 10 selection episodes per generation. Panel B: Inflation factor

698 as a function of the number of selection episodes. Panel C: Inflation factor as a function of the duration of the selection

699 window relative to the generation time α. Dotted lines (panel A) correspond to the autocorrelation of the environment

700 (θ) alone over g generations: ρ^{gT}.Crosses show results from simulations with a strength of stabilizing selection that

701 varies across selection episodes, while lines show the expectation assuming constant selection strength with same

702 mean (full lines: exact prediction using eq. 12, dashed lines: prediction for continuous selection along each generation

703 – infinite number of selection episodes, eq. 15). Numerical simulations are performed using eq. (10), with θ_{tot} and

704 ω_{tot}^2 calculated as described in eq. 3 from phenotypic optima θ_i and corresponding strengthes of selection ω_i^2

705 corresponding to each episode of selection i per generation as described in the following: for each episode of selection,

706 a phenotypic optimum is drawn from equation 11 and the strength of selection is drawn independently in a Gaussian

707 with mean $\sqrt{\omega_{tot}^2/n - 1}$ and variance 1. Total selection per generation thus follows a non-central χ^2 with mean ω_{tot}^2

708 and variance $4\omega_{tot}^2 - 2n$. For simulations, we kept the expected total strength of selection constant (independent on

709 the number of selection episode) to isolate the effect of the number of selection episodes from that of the total strength

710   of selection. For A and B, $\alpha = 0.8$. For all panels: light gray to black: $\rho^T = 0.2$, 0.5 and 0.9 respectively, $\bar{\omega}_{tot}^2 = 25$,

711    $\sigma_\theta^2 = 1$.

712

713   Figure 3: Variance of the selection gradient as a function of the number of selection episode per generation (A) and

714   of the autocorrelation of the environment (B). Panel A: environmental autocorrelation over a generation time is $\rho^T =$

715   0.5 (dark gray) and $\rho^T = 0.2$ (light gray), for two total strengths of selection per generation ($\bar{\omega}_{tot}^2 = 25$ [lower two

716   sets of simulations/expectations] and 10 [upper sets]). Panel B represents the variance of the total selection gradient

717   as a function of the autocorrelation of the environment, for the same two total strengths of selection, and $n = 10$.

718   Crosses represent results from numerical simulations where the strength of stabilizing selection varies across selection

719   episodes, whereas circles represent constant strength of stabilizing selection, as described in the caption of figure 2.

720   The dashed lines correspond to the predictions from eq. (16). Continuous lines represent predictions derived from a

721   continuous time approximation as in Lande and Shannon (1996, eq. 7), resulting in equation 5a in Chevin and Haller

722   (2014): $\mathrm{Var}[\beta_{tot}] = \mathrm{Var}[\theta_{tot}]S_{tot}^2 /(1 + S_{tot}G_0T_\theta)$, where T_θ is the characteristic time scale of the autocorrelation of

723   the environment (from eq. 13, and see eq. 11 and below). For both panels: $\alpha = 1$ and $\sigma_\theta^2 = 1$.

724

725   Figure 4: Autocorrelation of βtot over a single generation as a function of the number of selection episodes (A) and

726   of the total strength of selection per generation ω_{tot}^2 (B). Crosses represent results from numerical simulations with

727   variable strength of stabilizing selection, whereas circles represent those with constant stabilizing selection, as

728   described in the caption of figure 2. Dashed lines: expectations using equation 18. Continuous lines: expectation for a

729   single selection episode (eq. 17). From light gray to black, $\rho^T = 0.1$, 0.5 and 0.9. Panel A: $\omega_{tot}^2 = 10$. Panel B: $n = 5$.

730   For both panels: $\alpha = 1$ and $\sigma_\theta^2 = 1$.
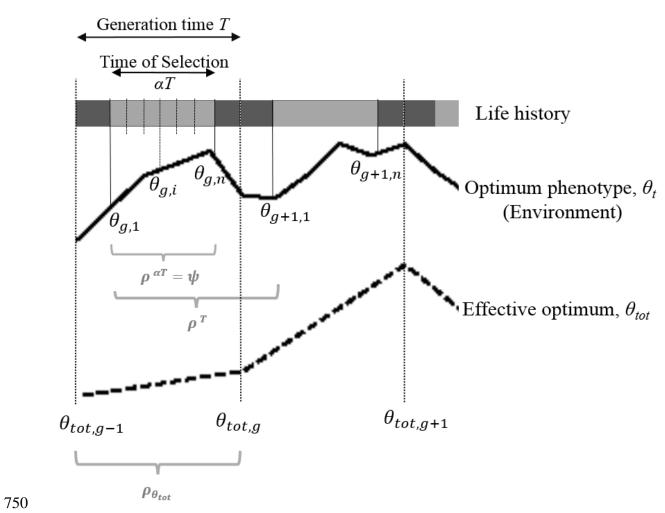
731

732   Figure 5: Autocorrelation function of βtot across generations. The embedded graph shows a detailed view of the first

733   five generations. Crosses represent results from numerical simulations with variable strength of stabilizing selection

734   whereas circles represent those with constant stabilizing selection, as described in the caption of figure 2. Dashed

735   lines: expectations using equation (18). Continuous lines: expectation for a single selection episode (eq. 17). Note that

736   for parameters shown here (number of selection episode and strength of selection) there is almost no difference

737   between simulations with deterministic (circles) and random (square) strength of selection per episode. From light

738   gray to black, $\rho^T = 0.1, 0.5$ and 0.9, $\omega_{tot}^2 = 10$, $\alpha = 1$ and $\sigma_\theta^2 = 1$.
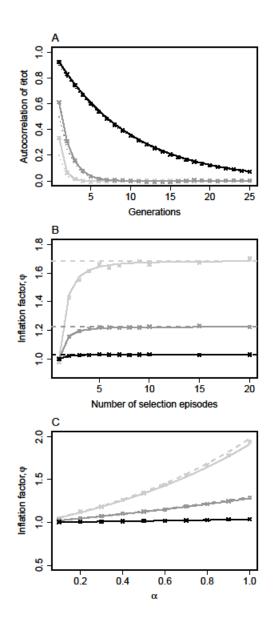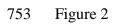
739

740   Figure 6: Maladaptation load as a function of the autocorrelation of the environment ρ^T (A) and as a function of the

741   number of selection episodes (B). Crosses represent results from numerical simulations with variable strength of

742   stabilizing selection whereas circles represent those with constant stabilizing selection, as described in the caption of

743   figure 2. The gray scale represents different number n of selection episodes per generation in panel A, and different

744   autocorrelation of the environment in panel B (light to dark gray, $\rho^T = 0.2, 0.5$ and 0.9). For both panels, $\bar{\omega}_{tot}^2 = 25$,
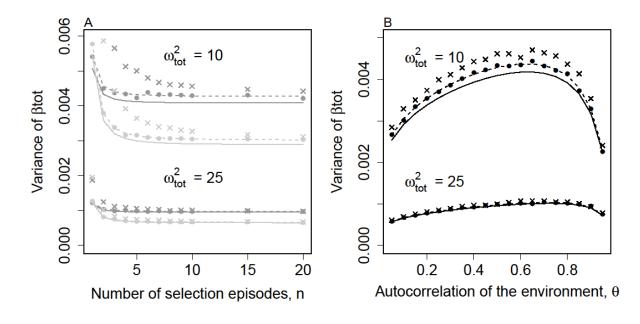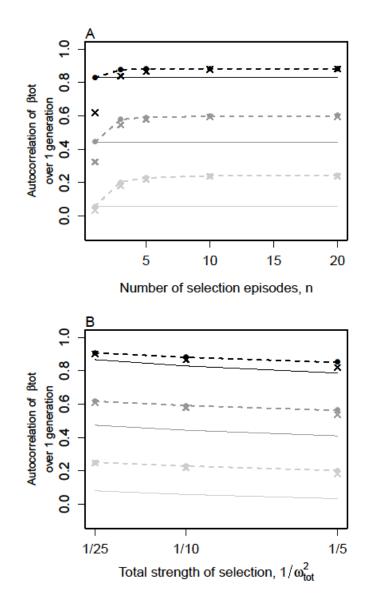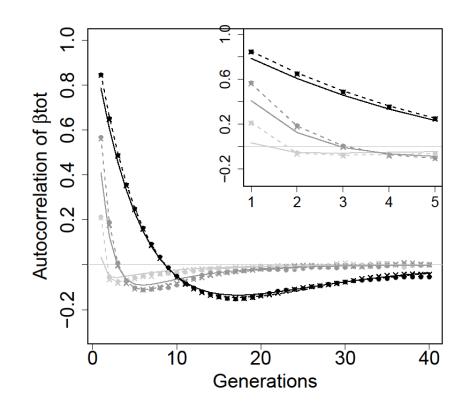
745    $\sigma_\theta^2 = 1$, $\alpha = 1$.

746

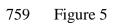747

35

749

750

751   Figure 1

752

753   Figure 2

754

755   Figure 3

756

757   Figure 4

758

759　　Figure 5

760

761   Figure 6

762

764   **Variance of the effective optimum**

765   By definition, the variance in the per-generation effective optimum is

766    $\text{Var}[\theta_{tot}] = Var[\sum_{k=1}^{n} e_k \theta_k] = \sigma_\theta^2 \sum_{k=1}^{n} e_k^2 + 2 \sum_{i=1}^{n-1} \sum_{j=i+1}^{n} cov[e_i \theta_i, e_j \theta_j],$ (A1)

767   where σ_θ^2 is the stationary variance of the per-episode optimum. Rewriting (A1) using the

768   properties of the autocorrelation of the environment (eq. 11) leads to

769    $\text{Var}[\theta_{tot}] = \sigma_\theta^2 (\sum_{k=1}^{n} e_k^2 + 2 \sum_{i=1}^{n-1} \sum_{j=i+1}^{n} e_i e_j \rho^{(j-i)\alpha T/n}),$ (A2)

770   with $e_i = \omega_{tot}^2 / \omega_i^2$. The first term in the right-hand side of equation (A2) corresponds to the direct

771   contribution of the variance of the environment. The second term on the right-hand side results

772   from the autocorrelation of the environment between selection episodes within a generation,

773   generating additional variation to the effective optimum. With the further assumption that the

774   strength of selection is the same at all episodes of selection, $\omega_i^2 = \omega^2,$ Equation A2 further

775   simplifies in

776    $\text{Var}[\theta_{tot}] = \sigma_\theta^2 \left(\frac{1}{n} + \frac{2}{n} \sum_{i=1}^{n-1} \sum_{j=i+1}^{n} \rho_\theta^{(j-i)\alpha T/n} \right) = \sigma_\theta^2 \frac{n - n\rho^{2\alpha T/n} + 2\rho^{\alpha T/n}(\rho^{\alpha T} - 1)}{n^2 (\rho^{\alpha T/n} - 1)^2}$ (A3)

777   The variance of the effective optimum θ_{tot} is always lower than the variance of the environment

778   (set to 1 in figure A1), and decreases with increasing number of selection episodes (fig A1-A).

779   However, $\text{Var}[\theta_{tot}]$ does not decrease without bounds, instead reaching a limit value for a large

780   number of episodes of selection, $\lim_{n\to\infty}(\text{Var}[\theta_{tot}]) = 2\frac{\psi - \ln\psi - 1}{(\ln\psi)^2}$, which only depend on the

781   autocorrelation of the environment over the time window for selection $\psi = \rho^{\alpha T}$. In addition, for

782   a given number of selection episodes, the variance of the effective optimum increases with the

783   autocorrelation of the environment (fig. A1-B).
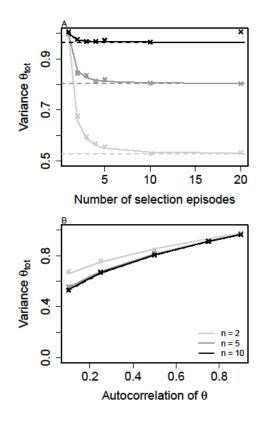
784

785

Figure A1: Variance of the effective optimum as a function of the number of selection episodes (A) and as a function
of the autocorrelation of the environment (B). Crosses represent the results from simulations where the strength of
selection is drawn from a probability distribution as described in fig. 2 caption. Full lines represent the expectation
from eq. A3 and dashed lines represent the limit for a large number of selection episodes. Panel A: from light grey to
dark $\rho_{\theta,T} = 0.2$, 0.5 and 0.9 respectively. Panel B: the gray scale represents different number of selection episode per
generation (see within the panel). For both panels, $\bar{\omega}_{tot}^2 = 25$, $\sigma_\theta^2 = 1$, $\alpha = 1$.

Variance of the selection gradient

The variance of β_{tot} is proportional to the variance of the distance of the mean phenotype to the

optimum

$$\text{Var}[\beta_{tot}] = (S_{tot})^2 \text{Var}[(\bar{z} - \theta_{tot})] = (S_{tot})^2 \text{E}[(\bar{z} - \theta_{tot})^2]. \tag{A4}$$

43

796   By rearranging equation 10 in the main text (Charlesworth 1993), the mean phenotypic value at

797   generation g is

798   $$\bar{z}_g = (1 - S_{tot}G_0)^g \bar{z}_0 + S_{tot}G_0 \sum_{i=1}^{g}(1 - S_{tot}G_0)^{i-1}\theta_{tot,g-i}. \tag{A5}$$

799   After a sufficiently large number of generations, the first term in equation (A5), corresponding to

800   the initial conditions, can be neglected. We thus obtain

801   $$\mathrm{E}[(\bar{z} - \theta_{tot})^2] = \mathrm{E}\left[\left(S_{tot}G_0 \sum_{i=1}^{g}(1 - S_{tot}G_0)^{i-1}\theta_{tot,g-i} - \theta_{tot,g}\right)^2\right], \tag{A6}$$

802   By developing terms, using the autocorrelation of the effective optimum (eq. 12) and assuming

803   that $g \to \infty$, we obtain equation (16) in the main text (see also Charlesworth 1993; eq. 19a)

804   $$\mathrm{Var}[\beta_{tot}] = 2\mathrm{Var}[\theta_{tot}]S_{tot}^2 \frac{1 - \rho(1 + S_{tot}G_0(\varphi - 1))}{(2 - S_{tot}G_0)(1 - \rho(1 - S_{tot}G_0))}.$$

805   **Autocorrelation of the selection gradient**

806   The autocovariance of the selection gradient over τ generations is

807   $$\mathrm{Cov}[\beta_{tot,g}, \beta_{tot,g-\tau}] = S_{tot}^2 \left(\mathrm{E}[\theta_{tot,g}\theta_{tot,g-\tau}] + \mathrm{E}[\bar{z}_g \bar{z}_{g-\tau}] - \mathrm{E}[\bar{z}_{g-\tau}\theta_{tot,g}] - \mathrm{E}[\theta_{tot,g-\tau}\bar{z}_g]\right). \tag{A7}$$

808   *Continuous time approach*

809   Following Lande and Shannon (1996), the dynamics can be approximated in continuous time. The

810   continuous time approximation eases the analysis. After long enough time so that the we can

811   neglect the initial conditions, the mean phenotype at time t is

812   $$\bar{z}_t = S_{tot}G_0 \int_0^\infty e^{-S_{tot}G_0 x}\theta_{tot,t-x}dx. \tag{A8}$$

813   Equation (A8) is the continuous time equivalent to equation (A6) once the effect of initial

814   conditions has been erased. From equations (A7) and (A8), the method to derive the

815 autocorrelation of the selection gradient is described in Chevin and Haller (2014, appendix for the

816 autoregressive optimum). This approach cannot a priori be used in the context of the present model

817 because the inflation factor is 1 for $\tau = 0$ and is not defined for $0 < \tau < 1$. However, we found

818 that the naïve approach to use equation (12) in the main text directly in the derivations from Chevin

819 and Haller (2014) matches closely the exact discrete time approach that we develop in the next

820 section. As we could not demonstrate this observation formally, we chose not to present this result

821 in our main text. We nevertheless provide this result here as a heuristic:

822 $$\rho_{\beta tot,\tau} = \varphi \frac{\rho^{\tau T} - S_{tot}G_0\frac{T_\theta}{T}e^{-S_{tot}G_0\tau}}{1 - S_{tot}G_0\frac{T_\theta}{T}}, \tag{A9}$$

823 where $\frac{T_\theta}{T}$ measures the characteristic timescale of the autocorrelation of the environment in units

824 of generation time.

825 *Discrete time approach*

826 In contrast with previous studies (Lande and Shannon 1996, Chevin and Haller 2014), we calculate

827 the autocorrelation of the selection gradient in discrete time. Similarly to the calculation for the

828 variance of the selection gradient, we use equation (A5) assuming that many generations occurred

829 so that the first term can be neglected. We also use equation (12) in the main text for the

830 autocorrelation of the effective optimum $\rho_{\theta tot,\tau} = \rho^{\tau T}\varphi$, reminding that $\varphi = 1$ for $\tau = 0$. The

831 general procedure follows Chevin and Haller (2014, appendix for the autoregressive optimum) by

832 calculating each expectation from equation (A7). Even though we kept notations concise, each

833 sum in the expectations below can be resolved exactly. The first expectation is straightforward

834 $$\mathrm{E}\big[\theta_{tot,g}\theta_{tot,g-\tau}\big] = \varphi\mathrm{Var}[\theta_{tot}]\rho^{\tau T}. \tag{A10}$$

835 The expectation for the first cross product is

836     $\mathrm{E}[\bar{z}_{g-\tau}\theta_{tot,g}] = S_{tot}G_0 \sum_{i=1}^{g-\tau}(1 - S_{tot}G_0)^{i-1}E[\theta_{tot,g}\theta_{tot,g-i-\tau}]$, taking into account the

837   discontinuity of the inflation factor I_f in $i = g - \tau$, it results in

838     $E[\bar{z}_{g-\tau}\theta_{tot,g}] = \varphi\mathrm{Var}[\theta_{tot}]S_{tot}G_0 \sum_{i=1}^{g-\tau-1}(1 - S_{tot}G_0)^{i-1}\rho^{(\tau+i)T} + S_{tot}G_0(1 -$

839     $S_{tot}G_0)^{g-\tau-1}\mathrm{Var}[\theta_{tot}]$.   (A11)

840   The expectation for second cross product is

841     $E[\theta_{tot,g-\tau}\bar{z}_g] = S_{tot}G_0 \sum_{i=1}^{g}(1 - S_{tot}G_0)^{i-1}E(\theta_{tot,g-i}\theta_{tot,g-\tau})$.

842   We need to distinguish 3 cases, $i < \tau$, $i > \tau$ and $i = \tau$:

843     $E[\theta_{tot,g-\tau}\bar{z}_g] = \varphi\mathrm{Var}[\theta_{tot}]S_{tot}G_0 \left(\sum_{i=1}^{\tau-1}(1 - S_{tot}G_0)^{i-1}\rho^{(\tau-i)T} + \sum_{i=\tau+1}^{g}(1 - \right.$

844     $\left. S_{tot}G_0)^{i-1}\rho^{(i-\tau)T} + \varphi^{-1}(1 - S_{tot}G_0)^{\tau-1} \right)$.   (A12)

845   Lastly,

846     $E[\bar{z}_g\bar{z}_{g-\tau}] = (S_{tot}G_0)^2 \sum_{i=1}^{g}\sum_{k=1}^{g-\tau}(1 - S_{tot}G_0)^{i+k-2}E[\theta_{tot,g-i}\theta_{tot,g-\tau-k}]$.

847   To calculate the double sum, it is convenient to perform a change of variables

848     $\sum_{i=1}^{g}\sum_{k=1}^{g-\tau}(1 - S_{tot}G_0)^{i+k-2}E[\theta_{tot,g-i}\theta_{tot,g-\tau-k}] = \sum_{i=1}^{g}\sum_{j=\tau+1}^{g}(1 -$

849     $S_{tot}G_0)^{i+j-\tau-2}E[\theta_{tot,g-i}\theta_{tot,g-j}]$.

850   We then need to distinguish 4 cases,

851   for $i < \tau+1$, $A = \varphi\mathrm{Var}[\theta_{tot}]\sum_{i=1}^{\tau}\sum_{j=\tau+1}^{g}(1 - S_{tot}G_0)^{i+j-\tau-2}\rho^{(j-i)T}$.

852   for $i > \tau$ and $i = j$, $B = \mathrm{Var}[\theta_{tot}] \sum_{i=\tau+1}^{g}(1 - S_{tot}G_0)^{2i-\tau-2}$.

853   for $i > \tau$ and $j > i$, $C = \varphi \mathrm{Var}[\theta_{tot}] \sum_{j=\tau+2}^{g} \sum_{i=\tau+1}^{j-1} (1 - S_{tot} G_0)^{i+j-\tau-2} \rho^{(j-i)T}$.

854   for $i > \tau$ and $i > j$, $D = \varphi \mathrm{Var}[\theta_{tot}] \sum_{i=\tau+2}^{g} \sum_{j=\tau+1}^{i-1} (1 - S_{tot} G_0)^{i+j-\tau-2} \rho^{(i-j)T}$,

855   with C = D, and resulting in

856     $E[\bar{z}_g \bar{z}_{g-\tau}] = (S_{tot} G_0)^2 (A + B + 2C).$ (A13)

857   Adding equations (A10) to (A13), finding the limit of this sum for large g, dividing by the

858   variance of the selection gradient (eq. 16) and rearranging leads to the autocorrelation of the

859   selection gradient

860     $\rho_{\beta tot, \tau} = \frac{\varphi \varepsilon \rho^{\tau T} + \gamma (1 - S_{tot} G_0)^{\tau}}{\vartheta},$ (A14)

861   where,

862     $\varepsilon = (\rho^T - 1)^2 (2 - S_{tot} G_0),$

863     $\gamma = \frac{S_{tot} G_0}{(1 - S_{tot} G_0)} \left(\rho^T (1 - \varphi)(S_{tot} G_0)^2 - (1 - \rho^T)(1 + \rho^T (2\varphi - 1))(1 - S_{tot} G_0) \right),$

864     $\vartheta = 2(\rho^T - 1 + S_{tot} G_0)(\rho^T - 1 + \rho^T (\varphi - 1) S_{tot} G_0).$

865   Equation (A14) is written in a form similar to equation (A9), decomposing the effects of the

866   autocorrelation of the environment and of the deviations of the mean phenotype to the optimum.

867   An interpretation for equation (A14) is proposed in the main text.

868   In the special case where there is a unique episode of selection per generation, i.e. $\varphi = 1$, equation

869   (A14) is

870     $\rho_{\beta tot, \tau} = \frac{\rho_{\theta}^{\tau T} - \kappa (1 - S_{tot} G_0)^{\tau}}{1 - \kappa},$ (A15)

871 where $\kappa = \frac{(1+\rho^T)S_{tot}\,G_0}{(1-\rho^T)(2-S_{tot}\,G_0)}$.

872 Equation (A15) is very similar to equation 5b in Chevin and Haller (2014). Comparing equation

873 (A14) and (A15) shows that the inflation factor, i.e. the autocorrelation of selection within

874 generation, complicates the analysis by introducing new terms at the interface between the

875 autocorrelation of the environment and the dynamics of selection within and across generations.

876 A Taylor expansion performed on the reciprocals of equation (A15) and 5b in Chevin and Haller

877 (2014) shows that both equations are identical to at least the second order. This result can be

878 confirmed by representing both functions for different autocorrelation of the environment. Both

879 functions match exactly on most of the autocorrelation range with minor deviation at very weak

880 autocorrelation (not shown).

881 **Changes in (co)variances under selection**

882 Here we derive the changes in the variances and covariances of phenotypic components after each

883 selection episode. Following classical quantitative genetics, we assume that the phenotype z of

884 any individual prior to any selection in a generation is the sum of two normally distributed

885 components: the breeding value x and environmental effect e. At the beginning of a generation,

886 these phenotypic components have means $\bar{x}$ and $\bar{e} = 0$, variances G and E, and are uncorrelated,

887 such that their covariance is $C_{x,e} = 0$ and the total phenotypic variance is $P = G + E$. Changes in

888 the mean breeding value under selection are obtained from changes in mean phenotype using the

889 regression of breeding values on phenotypes, which at the beginning of a generation has slope

890 $\frac{\text{Cov}(x,z)}{P} = \frac{G}{G+E} = h^2$, following the usual notation for heritability.

891 We consider episodes of selection caused by a Gaussian fitness peak, such that individuals with

892 phenotype z have fitness $(z) \propto \exp(-\frac{(z-\theta)^2}{2\omega^2})$ (where we omit indices for selection episodes and

893 generation for simplicity). It is informative to start by investigating the first selection episode in a

894 generation, where x and e are independent and $\bar{e} = 0$, $\bar{z} = \bar{x}$. The fitness function on breeding

895 values is obtained by integrating over the distribution of environmental effects, $\widetilde{W}(x) \propto$

896 $\exp\left(-\frac{(x-\theta)^2}{2(\omega^2+E)}\right)$, and the fitness function on environmental effects is obtained similarly by

897 integrating over breeding values, $W_e(e) \propto \exp(-\frac{(\bar{x}+e-\theta)^2}{2(\omega^2+G)})$. The fitness function on breeding

898 values (respectively, on environmental effects) is thus also Gaussian, with squared width $\omega^2 + V_e$

899 (respectively $\omega^2 + G$) and optimum θ (respectively $\theta - \bar{x}$). With a Gaussian fitness peak, the

900 distribution of phenotypes, breeding values and environmental effects after selection remain

901 Gaussian. Denoting the per-episode strength of stabilizing selection as $S = \frac{1}{\omega^2+P}$, the means after

902 selection are

903 $$\bar{z}^* = \theta + \frac{\omega^2}{\omega^2+P}(\bar{z} - \theta) = \theta + (1 - SP)(\bar{z} - \theta) = \bar{z} - SP(\bar{z} - \theta) \tag{A16a}$$

904 $$\bar{x}^* = \theta + \frac{\omega^2+V_e}{\omega^2+P}(\bar{x} - \theta) = \theta + (1 - SG)(\bar{x} - \theta) = \bar{z} - SG(\bar{z} - \theta) \tag{A16b}$$

905 $$\bar{e}^* = \theta - \bar{x} + \frac{\omega^2+G}{\omega^2+P}(\bar{x} - \theta) = \theta - \bar{x} + (1 - SE)(\bar{x} - \theta) = -SE(\bar{z} - \theta), \tag{A16c}$$

906 where we have used the fact that $\bar{e} = 0$ and thus $\bar{z} = \bar{x}$ prior to any selection. Note that $\bar{x}^* - \bar{x} =$

907 $h^2(\bar{z}^* - \bar{z})$ and $\bar{e}^* - \bar{e} = (1 - h^2)(\bar{z}^* - \bar{z})$, as required. The variances after selection are

908 $$P^* = \left(\frac{1}{\omega^2} + \frac{1}{P}\right)^{-1} = (1 - SP)P \tag{A17a}$$

909 $$G^* = \left(\frac{1}{\omega^2+E} + \frac{1}{G}\right)^{-1} = (1 - SG)G \tag{A17b}$$

49

910     $E^* = \left(\frac{1}{\omega^2+G} + \frac{1}{E}\right)^{-1} = (1 - SE)E,$ (A17c)

911   which satisfy the relationships $G^* - G = h^4(P^* - P)$ and $E^* - E = (1 - h^2)^2(P^* - P)$. The

912   phenotypic variance after selection must also satisfy

913     $P^* = G^* + E^* + 2\,C_{x,e}^*$ (A18)

914   so the covariance of breeding values and environmental effects after selection is

915     $C_{x,e}^* = \frac{P^* - G^* - E^*}{2}.$ (A19)

916   Using $P = G + E$ this yields

917     $C_{x,e}^* = \frac{(1-SP)P - (1-SG)G - (1-SE)E}{2} = -S\frac{P^2 - G^2 - E^2}{2} = -SGE,$ (A20)

918   which satisfies $C_{x,e}^* = C_{x,e}^* - C_{x,e} = h^2(1 - h^2)(P^* - P)$.

919   These formulas apply to the first selection episode, but in further episodes the change in the mean

920   breeding value and environmental effects also depend on their covariance. More general formulas

921   for change at any selection episode can be derived through a multivariate approach. Let us denote

922   the vector of breeding values and environmental effects as $\mathbf{y} = (x, e)^{\mathrm{T}}$ (where superscript T

923   denotes a transposition), with mean $\bar{\mathbf{y}}$ and covariance matrix $\mathbf{Y}$. Substituting $x + e$ for z in the

924   fitness function $W(z)$, and integrating over the joint distribution of x and e, the mean fitness is

925     $\bar{W} \propto \exp\left(-\frac{S_C\,(\bar{x}+\bar{e}-\theta)^2}{2}\right)$ (A21)

926     $S_C = \frac{1}{\omega^2 + G + E + 2C_{x,e}}$ (A22)

927   Then using standard results from evolutionary quantitative genetics (Lande 1979, 1980, Lande and

928   Arnold 1983) and properties of the Gaussian function, the change in the vector of mean breeding

929   values and environmental effects under selection within a generation is

930   $$\Delta^*\bar{\mathbf{y}} = \mathbf{Y}\partial_{\bar{\mathbf{y}}}\ln\bar{W} \tag{A23}$$

931   where $\partial_{\bar{\mathbf{y}}}$ is the vector of partial derivatives with respect to each element of $\bar{\mathbf{y}}$, yielding

932   $$\Delta^*\bar{x} = -S_C(\bar{x} + \bar{e} - \theta)(G + C_{x,e}) \tag{A24a}$$

933   $$\Delta^*\bar{e} = -S_C(\bar{x} + \bar{e} - \theta)(E + C_{x,e}) \tag{A24b}$$

934   $$\Delta^*\bar{z} = \Delta^*\bar{x} + \Delta^*\bar{e} = -S_C(\bar{x} + \bar{e} - \theta)(G + E + 2C_{x,e}) \tag{A24c}$$

935   When $\bar{e} = C_{x,e} = 0$, these simplify to $\Delta^*\bar{x} = -SG(\bar{x} - \theta)$ and $\Delta^*\bar{e} = -SE(\bar{x} - \theta)$, consistent

936   with the formulas above for the first episode of selection. The recursion for the covariance matrix

937   is

938   $$\Delta^*\mathbf{Y} = \mathbf{Y}(\partial^2_{\bar{\mathbf{y}}}\ln\bar{W})\mathbf{Y} \tag{A25}$$

939   where $\partial^2_{\bar{\mathbf{y}}}$ is the Hessian matrix of second partial derivatives with respect to each element of $\bar{\mathbf{y}}$,

940   yielding

941   $$\Delta^*G = -S_C(G + C_{x,e})^2 \tag{A26}$$

942   $$\Delta^*E = -S_C(E + C_{x,e})^2 \tag{A27}$$

943   $$\Delta^*C_{x,e} = -S_C(G + C_{x,e})(E + C_{x,e}) \tag{A28}$$

944   When $\bar{e} = C_{x,e} = 0$, these simplify to $\Delta^*G = -SG^2$, $\Delta^*E = -SE^2$, and $C_{x,e} = -SGE$, again

945   consistent with the formulas above for the first episode of selection.

946 In the general case where $\bar{e}$ and $C_{x,e}$ are non-zero, as is expected if the population has previously

947 undergone any episode of selection in the ongoing generation, then the relationship between

948 phenotypic change and change in breeding values cannot be inferred directly from current

949 components of phenotypic variance. Indeed we have

950 $$\frac{\Delta^*\bar{x}}{\Delta^*\bar{z}} = \frac{G+C_{x,e}}{G+E+2C_{x,e}} = \frac{\text{Cov}(x,x+e)}{\text{Var}(x+e)} \tag{A29}$$

951 which is still a regression slope of breeding values on phenotypes, but this no longer translates into

952 a ratio of additive genetic variance on phenotypic variance, because of the covariance between

953 breeding values and environmental values. However, it can be shown that this ratio always equals

954 the ratio $\frac{G}{G+E} = h^2$ at the beginning of a generation.

955 **References**

956

957 Charlesworth, B. 1993. Directional selection and the evolution of sex and recombination. Genetics

958   Research **61**:205-224.

959 Chevin, L. M., and B. C. Haller. 2014. The temporal distribution of directional gradients under

960   selection for an optimum. Evolution **68**:3381-3394.

961 Lande, R. 1979. Quantitative genetic analysis of multivariate evolution, applied to brain: body size

962   allometry. Evolution **33**:402-416.

963 Lande, R. 1980. Sexual dimorphism, sexual selection, and adaptation in polygenic characters.

964   Evolution **34**:292-305.

965 Lande, R., and S. J. Arnold. 1983. The measurement of selection on correlated characters.

966   Evolution **37**:1210-1226.

967　　Lande, R., and S. Shannon. 1996. The role of genetic variation in adaptation and population

968　　　　　persistence in a changing environment. Evolution **50**:434-437.

969

970